Journal of ELECTRONIC MATERIALS, Vol. 46, No. 12, 2017
DOI: 10.1007/s11664-017-5731-2

Ab Initio High Pressure and Temperature Investigation on Cubic $PbMoO_3$ Perovskite

SAJAD AHMAD DAR,[1,4] VIPUL SRIVASTAVA,[2] and UMESH KUMAR SAKALLE[3]

1.—Department of Physics, Govt. Motilal Vigyan Mahavidyalya College, Bhopal, MP 462008, India. 2.—Department of Physics, NRI Institute of Research and Technology, Bhopal, MP 462021, India. 3.—Department of Physics, S. N. P. G. College, Khandwa, MP 450001, India. 4.—e-mail: sajad54453@gmail.com

A combined high pressure and temperature investigation on recently reported cubic perovskite $PbMoO_3$ have been performed within the most accurate density functional theory (DFT). The structure was found stable in cubic paramagnetic phase. The DFT calculated analytical and experimental lattice constant were found in good agreement. The analytical tolerance factor as well as the elastic properties further verifies the cubic stability for $PbMoO_3$. The spin polarized electronic band structure and density of states presented metallic nature with symmetry in up and down states. The insignificant magnetic moment also confirms the paramagnetic nature for the compound. The high pressure elastic and mechanical study up to 35 GPa reveal the structural stability of the material in this pressure range. The compound was found to establish a ductile nature. The electrical conductivity obtained from the band structure results show a decreasing trend with increasing temperature. The temperature dependence of thermodynamic parameters such as specific heat (C_v), thermal expansion (α) has also been evaluated.

Key words: *Ab-Initio* calculations, high temperature, high pressure, electronic, thermodynamics, elastic and mechanical properties

INTRODUCTION

Material science has always remained in search of new, reliable and cost effective materials having a wide range of applications and featuring marvelous properties. Among these materials, perovskites have gained significant attention, because of their wide range of physical properties, simple structure, accommodation of the majority of elements from the periodic table and the abundance of these materials on earth's crust. These materials have displayed so many interesting and fascinating properties like multiferrocity[1,2] spintronics,[3,4] ionic conductivity, piezoelectricity ferroelectricity.[5–7] With the fast rate of decline of fossil fuel reserves, an increase in global warming perovskites is being thoroughly investigated for fuel cell applications as a substitute for these fossil fuels. These materials have been part of many high tech devices.[8]

Transition metal-based perovskites are being considered as important candidates for electrode materials.[9–11] Takatsu et al.[12] has recently reported $PbMoO_3$ in cubic structure with space group Pm-3m (221), having anomalous metallic behavior and different from the lead (Pb)-based perovskites, which are usually distorted. Mo-based perovskites such as $SrMoO_3$, $BaMoO_3$ and $CaMoO_3$ have been extensively studied both experimentally and theoretically.[13–15] These perovskites with a metallic nature and paramagnetic properties have generally good electrical conductivity and hardness, which have made them as the promising candidates for electrode materials in fuel cells.[16,17] This is because in electronics the fabrication of electrode materials should have low electrical resistance; materials like

(Received June 23, 2017; accepted July 29, 2017; published online August 11, 2017)

$SrRuO_3$, $BaMoO_3$[7–11] and $SrMoO_3$[18] have been widely used in electrode materials.

Paramagnetic Pb-based perovskites $PbMoO_3$ have been reported to crystalize in cubic B2 phase, Pm-3m (221) space group with a lattice constant of 3.999 Å.[12] Not much is known about this compound, but similar compounds such as that of $PbMoO_3$ are reported like $MTaO_3$ (M = Ca, Sr and Ba)[19] and $PbTaO_3$.[20] Thus, in this paper we made an attempt to predict the properties for $PbMoO_3$ and to overcome the lack of data. This data may serve as a reference for the future advance in experimental and theoretical studies for $PbMoO_3$.

In this study structural, elasto-mechanical, thermo-electronic and thermodynamic properties of perovskite oxides $PbMoO_3$ have been investigated under pressure and temperature. Pressure and temperature plays an important role in decoration of the material properties. The study has been accomplished with the successful density functional theory (DFT),[21] quasi harmonic model Debye approximation[22,23] and Boltztrap code.[24,25]

COMPUTATIONAL METHODS

The computation has been carried by solving Kohn–Sham equations in order to obtain structural electronic and magnetic properties of $PbMoO_3$. The full-potential linear augmented plane wave (FP-LAPW) method within the density functional theory (DFT)[27] as implemented in WIEN2K[26] has been used within a generalized gradient approximation GGA of (Perdew-Burke-Ernzehof),[27] GGA + U,[28] modified Becke Johnson mBJ[29] and spin–orbit coupling GGA + U + SOC.[30] For GGA + U certain values for U have been tested, as to accommodate Mo-d and Pb-f orbitals in the density of states, and the final value U was set to 2.50 eV and J was set to 0, $U_{\text{eff}} = U - J$.[19] The unit cell is divided into non-overlapping spheres centered at atomic sites of radius and an interstitial region. The basic set inside each muffin tin sphere is divided into core and valence states. The core states are treated within the spherical part of the potential only and are assigned to have spherical symmetric charge density restricted within the muffin tin spheres. To obtain the energy convergence, the basic functions are expanded up to $R_{\text{MT}}K_{\text{max}} = 7.5$, where R_{MT} is the smallest atomic radius in the unit cell and K_{max} denotes the scale of the major **k** vector in the plane wave expansion. The value of $l_{\text{max}} = 10$, refers to the maximum value of angular momentum for partial waves inside the atomic sphere. The charge density is Fourier expanded up to $G_{\text{max}} = 12$ (a.u.)$^{-1}$. The self-consistent calculations converge when the total energy of the system is stable within 10^{-4} Ry. The energy separation between the core states and valence states is set to −6.0 Ry. The dependence of total energy on the number of K-points in the irreducible wedge of the first brillouin zone (BZ) has been expanded within the linearized tetrahedron[31] scheme by performing the calculations for 1500 K-points.

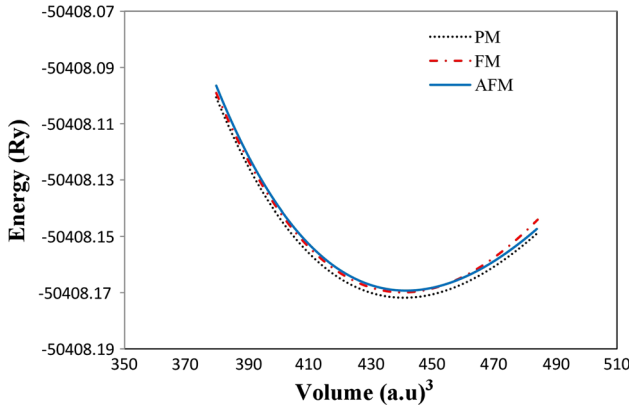

Fig. 1. Energy with respect to volume for ferromagnetic (FM), paramagnetic (PM) and anti-ferromagnetic (AFM) phase of $PbMoO_3$.

The elastic constants have been calculated by Charpin's method[32] as implemented in WIEN2K under high pressure and from these elastic constants other mechanical properties like Young's modulus, Shear modulus, etc., have been calculated in the pressure range of 0 GPa to 35 GPa. For the study of thermodynamic properties, a quasi harmonic Debye model has been used. The results obtained from band structure calculations have been fetched to Boltzmann transport theory to evaluate and to check the temperature dependence of electrical conductivity.

RESULTS AND DISCUSSION

Structural Properties

PbMoO3 perovskite crystalizes in cubic phase with space group 221 (Pm-3m).[12] The atoms are positioned in such a way that Pb lies at the corners (0, 0, 0), Mo at the center (0.5, 0.5, 0.5) and O atoms are held at face centers (0.5, 0.5, 0), (0.5, 0, 0.5), (0, 0.5, 0.5) of cubic unit cells. The geometry and structural properties of cubic $PbMoO_3$ have been studied using the Birch-Murnaghan[33] equation of state by fitting the total energy as a function of unit cell volume in ferromagnetic (FM), paramagnetic (PM) and anti-ferromagnetic (AFM) cases within GGA. The ground state energy was found to be a minimum for the paramagnetic phase as presented in Fig. 1 and, hence, is a stable configuration. The ground state parameters such as bulk modulus, lattice constant and pressure derivatives in FM, PM and AFM cases are grouped in Table I.

The lattice constant for PbMoO3 has also been calculated analytically from the ionic radius of the individual elements using Eq. 1.[34]

$$a_0 = \alpha + \beta(r_{\text{Pb}} + r_{\text{O}}) + \gamma(r_{\text{Mo}} + r_{\text{O}}), \qquad (1)$$

where α, β, γ are constants equal to 0.06741, 0.4905 and 1.2921, respectively, and the ionic radii are $r_{\text{Pb}}(1.40)$, $r_{\text{Mo}}(0.59)$ and $r_{\text{O}}(1.35)$.[35] The experimental

Table I. Calculated value of lattice constant (a_0), bulk modulus (B_0), and pressure derivative (B) under the GGA scheme

$PbMoO_3$	GGA	Exp.	Ionic radius method
a_0 (Å)	4.027	3.99[12]	3.95
B(GPa)	188		
B'	4.53		
t	1.00		1.00
Bond length			
Pb-O (Å)	2.847		
Pb-Mo (Å)	3.487		
Mo-o (Å)	2.013		

lattice constant and that obtained by the analytical method and DFT show a close resemblance. Tolerance factor, which is an important parameter for the description of symmetry of perovskite compounds, have also been calculated by the well-known Goldschmidt's formula[36] from the ionic radius and has also been obtained from the bound length data for $PbMoO_3$.

$$t = \frac{0.707(r_{Pb} + r_O)}{(r_{Mo} + r_O)} \tag{2}$$

$$t = \frac{0.707(\langle Pb - O\rangle)}{(\langle Mo - O\rangle)} \tag{3}$$

where $\langle Pb - O\rangle$ and $\langle Mo - O\rangle$ are the average bound lengths between Pb-O and Mo-O.

The calculated values of the tolerance factor from both Goldschmidt's formula and bond length data properly follow the criteria for cubic symmetry (0.93–1.04)[37,38] and are grouped in Table II.

Elastic and Mechanical Properties

The structural stability and mechanical properties of cubic $PbMoO_3$ have been obtained from the knowledge of elastic stiffness constants C_{IJ} values. For a cubic system, the symmetry is in such a way that 21 elastic constants are reduced to three independent elastic constants C_{IJ} (C_{11}, C_{12}, C_{44}). The value of these elastic constants has been obtained by the Charpin method as implemented in WIEN2K by calculating the total energy as a function of volume-conserving strains. The study of elastic properties for the compound has been carried in the pressure range of 0 GPa to 35 GPa. The calculated C_{IJ} values in this pressure range properly satisfy the criteria for cubic elastic constants and ensure the stability C_{11}–$C_{12} > 0$, $C_{11} > 0$, $C_{44} > 0$, $(C_{11} + 2C_{12}) > 0$, $C_{12} < B < C_{11}$.[39] Thus, from the above criteria, the material is elastically stable in the pressure range of 0 GPa to 35 GPa.

Mechanical properties deal with the strength of the material and provide an insight in understanding the application of a particular material. In this study the mechanical properties like shear modulus (G); Young's modulus (Y), Poisson's ratio (v) and anisotropic factor (A) have been calculated and discussed. Shear modulus helps in knowing the plastic deformation of the material. Hills Shear modulus (G) has been defined as the arithmetic mean of Voigt (G_V) and Reuss (G_R)[40,41] values, which are represented as the upper and lower limits given by Eqs. 4 and 5

$$G_V = \frac{1}{5}(C_{11} - C_{12} + 3C_{44}), \tag{4}$$

$$G_R = \frac{5(C_{11} - C_{12})C_{44}}{3(C_{11} - C_{12}) + 4C_{44}}. \tag{5}$$

The value of (G) obtained at different pressure points indicates an increasing trend with the lowest value of 46 GPa at 0 GPa of pressure and the highest value of 103 GPa at 35 GPa pressure. Young's modulus (Y) deals with the stiffness of the material. The value of (Y) is calculated using Eq. 6

$$Y = \frac{9BG}{3B + G}. \tag{6}$$

The calculated value of (Y) at different pressure points is found to increase from 129 GPa at 0 GPa pressure to 281 GPa at 35 GPa pressure. The rigidity of the material is usually presented by the value of the bulk modulus (B). The calculated value of (B) shows an increase in the material rigidity, the value shows an increasing trend with the value of 187 GPa at 0 GPa of pressure and 341 GPa at 35 GPa of pressure. Thus, the large and increasing values of (B) and (Y) provides the indication that the stiffness and hardness of the material increases as the pressure is increased, and; hence, PbMoO3 may be a best candidate for the fabrication of ultra-hard materials.

The Pugh ratio's (B/G) offers evidence on ductility and brittleness of a material. According to Pugh,[42] a material is brittle if the (B/G) <1.75 and is ductile otherwise. The calculated B/G ratio is higher than the limit value at all the pressure points, and; hence, $PbMoO_3$ will behave as ductile material. This ductility is further verified from the Cauchy pressure (C_{12}–C_{44}), According to this, a material is

ductile if (C_{12}–C_{44}) is positive or otherwise ductile. The large and positive value of (C_{12}–C_{44}) at all the pressure points indicates that the material stays ductile even when the pressure is increased. Zener's anisotropy factor '*A*' is the property of a material to show altered characteristics in different directions of its structure, if '*A*' factor has unit value, the material is isotropic or otherwise anisotropic. The value of anisotropy is determined by

$$A = \frac{2C_{44}}{C_{11} - C_{12}}. \tag{7}$$

The calculated value of '*A*' at all the pressure values is less than unity and, hence, will have an anisotropic nature.

Another property called Poisson's ratio (v) has been calculated that helps us to know the nature of bonding forces. The Poisson's ratio (v) has been calculated by using the expression (8).

$$v = \frac{3B - 2G}{2(3B + G)} \tag{8}$$

The upper and lower and limits of Poisson's ratio are 0.25 and 0.50.[43] The (v) value varies from material to material. For covalent materials, (v) has a typical value of 0.1, for ionic materials (v) = 0.25 and for metallic materials the value is 0.25 to 0.50. The values of (v) for $PbMoO_3$ 0 GPa of pressure to 35 GPa were found in the range of 0.35 to 0.38 and, thus, suggests a high metallic behavior as inter-atomic bonding.

Debye temperature (θ_D), a very important thermodynamic parameter, gives valuable information on the performance of heat capacity for solids. One of the methods to estimate Debye temperature (θ_D) is from the average sound velocity (v_m) by the following equation[44]

$$\theta_D = \frac{h}{k_B}\left[\frac{3}{4\pi V_a}\right]^{1/3} v_m, \tag{9}$$

where h is the Plank's constant, K_B is Boltzmann's constant and V_a is the average atomic volume. The average wave velocity is given by (v_m) and is determined by the following relation:

$$v_m = \left[\frac{1}{3}\left(\frac{2}{v_t^3} + \frac{1}{v_l^3}\right)\right]^{-\frac{1}{3}}, \tag{10}$$

where v_l is the longitudinal elastic wave velocity and v_t is the transverse elastic wave velocity and these are given by the following relations.[44]

$$v_t = \left(\frac{G}{\rho}\right)^{\frac{1}{2}} \tag{11}$$

$$v_l = \left(\frac{3B + 4G}{3\rho}\right)^{\frac{1}{2}} \tag{12}$$

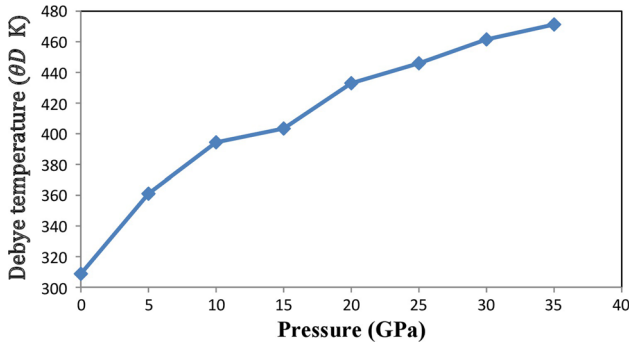

Fig. 2. Debye temperature (θ_D) as a function of pressure for $PbMoO_3$.

The calculated values of Debye temperature for PbMoO3 at 0 GPa and 35 GPa are 308.8 K and 472.21 K, respectively. The variation of Debye with respect to pressure is shown in Fig. 2, which shows that Debye temperature increases as the pressure is increased. From the knowledge of the elastic constants, another important thermodynamic quantity, known as the melting temperature, has been determined using Eq. 13 given by[45];

$$T_m(K) = [553(\mathrm{K}) + (5.911)C_{12}]\mathrm{GPa} \pm 300\,\mathrm{K}. \tag{13}$$

The calculated value of melting temperatures and all other elastic, mechanical and thermal properties at different pressure points are grouped in Table II.

Electronic and Magnetic Properties

For electronic study; band structure and density of states usually present a pictorial representation of the materials electronic potential. Spin polarized band structure and density of states have been calculated and plotted using GGA computed lattice constant via different methods (GGA, GGA + U, mBJ, GGA + U + SOC). The total density of states (TDOS) for $PbMoO_3$ plotted in Fig. 3 clearly presents a 0% of spin polarization for up and down states. The symmetric density for up and down states and the occupation of the Fermi level in all the methods shows the metallic nature of the compound with a small difference in the density of states. Figure 3 clearly indicates that (density of states) DOS using GGA, GGA + U and including spin orbit coupling GGA + U + SOC are almost similar, while in case of mBJ, the DOS present at −1.62 eV inside the valance band is pulled by the conduction band to −0.67 eV, but the overall DOS shows the metallic nature in all the four methods. The (TDOS) plot can be divided into two regions; one stretching inside the valence band from −10 eV to −3.06 eV, and another region stretches from −1.68 eV present in the valence band to 10 eV inside the conduction band. The calculated band structure within GGA + U (Fig. 4) also elucidates

Table II. Calculated elastic constants C_{11}, C_{12}, C_{44} in (GPa), bulk modulus B GPa, shear modulus G (GPa), Young's modulus Y (GPa), Poisson's ratio ν, Zener anisotropy factor A, B/G ratio, Cauchy pressure (C_{12}–C_{44}), density ρ (g/cm^3), longitudinal, transverse and average sound velocity (v_l, v_t, v_m, respectively, in m/s), melting temperature T_m (K) ± 300 K and Debye temperature (θ_D in K) for $PbMoO_3$ under pressure (GPa)

GGA (approx)	0 GPa	5 GPa	10 GPa	15 GPa	20 GPa	25 GPa	30 GPa	35 GPa
C_{11}	301	352	391	424	480	525	554	607
C_{12}	130	137	146	163	164	176	185	190
C_{44}	30	37	47	49	55	57	63	61
B	187	211	231	255	276	300	318	341
G	46	58	69	73	85	91	98	103
Y	129	159	190	201	232	248	266	281
ν	0.3850	0.3741	0.3624	0.3686	0.3598	0.3622	0.3602	0.3626
B/G	4.0161	3.639	3.3197	3.493	3.233	3.29	3.24	3.30
C_{12}–C_{44}	99.8	99.96	99	114	109	119	122	128
A	0.3523	0.3499	0.3833	0.3754	0.3470	0.4135	0.3410	0.2926
ρ	8.927	9.18	9.36	9.56	9.75	9.92	10.08	10.24
V_l	5011.77	5605.38	5891.01	6047.59	6323.04	6523.28	6716.25	6835.66
V_t	2285.02	2513.57	2730.99	2771.83	2958.86	3031.54	3118.04	3173.90
V_m	2445.38	2835.22	3074.86	3122.71	3330.17	3414.02	3510.49	3573.64
T_m	2335	2639	2865	3059	3393	3661	3830	4143
θ_D	308.8	361.07	394.4	403.4	432.98	446	461.56	472.31

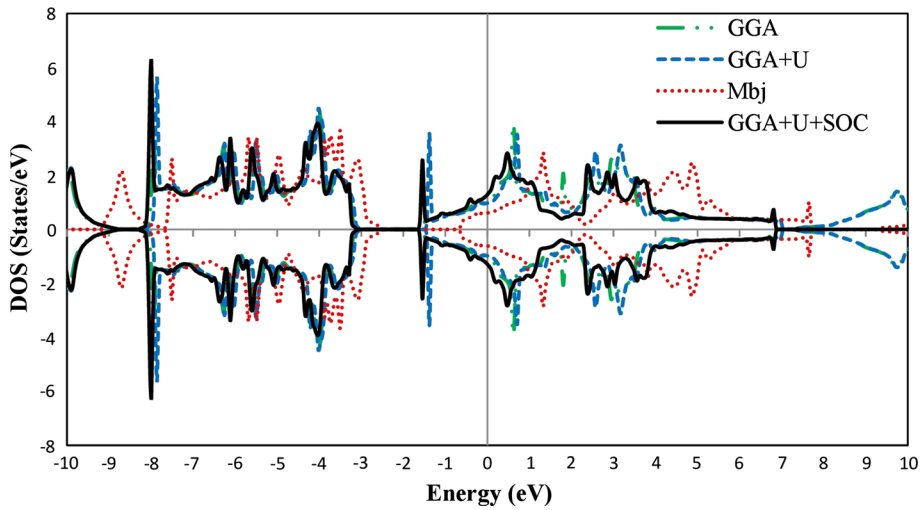

Fig. 3. Total density of states for spin up and down for $PbMoO_3$ within GGA, GGA + U, GGA + U + SOC and mbj.

the crossing over of bands at Fermi-level and, hence, a metallic nature. Furthermore, to have a proper understanding of band origin, a partial density of states has been calculated for Pb-p, f, d Mo-p, d and O-s, p within GGA + U and depicted in Fig. 5. The contribution to DOS in the valance band −10 eV to −3.18 eV is mainly due to Mo-d and O-p states with the highest density at −4.2 eV from O-p states. The second region, which is present at −1.68 eV to 10 eV, is highly occupied by Mo-d and Mo-p states with a small contribution of O-p states hybridized with one another. The maximum density in this region is in the vicinity of the Fermi level at −1.49 eV due to Mo-d states. Hence, the complete band description and density of states clearly indicate the metallic nature of $PbMoO_3$ and also shows symmetry for up and down states.

Magnetism in materials plays a vital role as to decide their interactions and proper applications. The magnetism in materials arises as a result of partially filled electron shells of atoms, while for those having completely filled electron shells, the moments cancel each other resulting in net zero magnetic moment.

The magnetic study has been carried out to check the overall magnetic nature using GGA, GGA + U, mBJ, and GGA + U + SOC. Different methods have been used to check the variation in results. The contribution of partial and interstitial moments to total magnetic moment was inspected. The

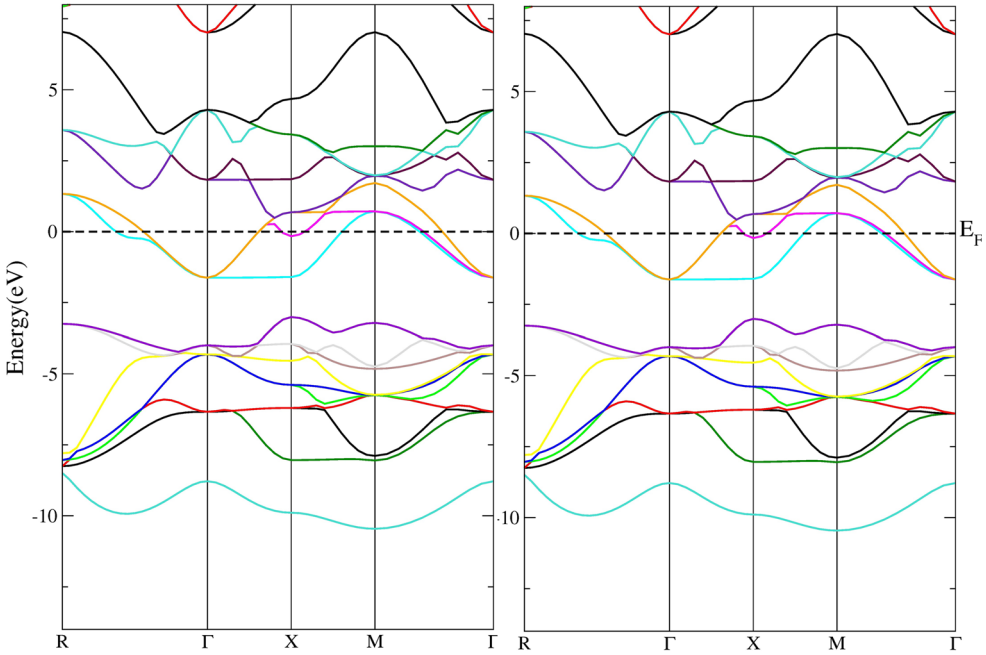

Fig. 4. Band structure of $PbMoO_3$ left spin up and right spin down states within GGA + *U*.

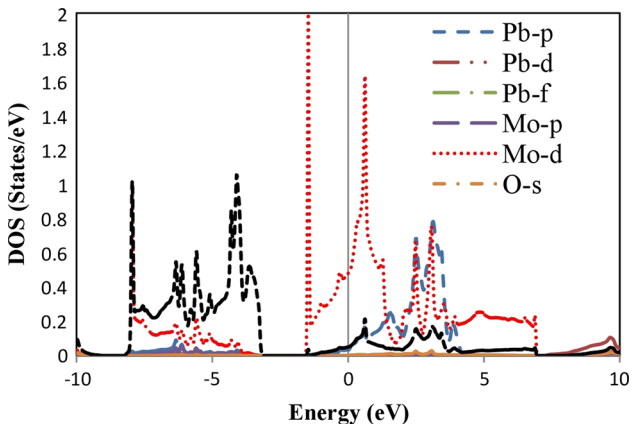

Fig. 5. Partial DOS contribution within GGA + *U*.

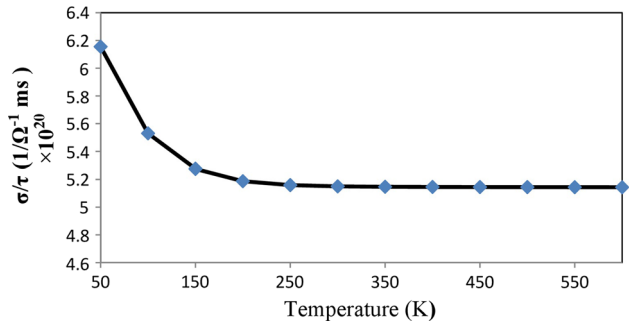

Fig. 6. Electrical conductivity as a function of temperature for $PbMoO_3$.

calculated values of total magnetic moments for $PbMoO_3$ are 0.00003 μ_B, 0.00001 μ_B, 0.00002 μ_B, and 0 μ_B, respectively, using GGA, GGA + *U*, mBJ, and GGA + *U* + SOC. Thus, symmetric density for up and down states, ground state energy and insignificant magnetic moment confirm the paramagnetic nature for $PbMoO_3$.

The effect on electrical conductivity with temperature has been finalized using post-DFT Boltztrap code.[24,25] Electrical conductivity is described as the number of free charge carrier flow. The electrical conductivity of metals decreases with increasing temperature as the increase in thermal motion restricts the flow of electrons inside the conduction band. The variation of electrical conductivity by time factor (*s*/*t*) with temperature is shown in Fig. 6 electrical conductivity for $PbMoO_3$ was found to be 6.16×10^{20} (ohm m)$^{-1}$ s^{-1} at 50 K of temperature and then a sharp decrease is observed up to 200 K and beyond 200 K, it is almost constant. Thus, the material shows significant electrical conductivity up to 500 K. For materials $CaTaO_3$, $SrTaO_3$, $BaTaO_3$[19] similar results have been reported like good electrical conductivity and metallic nature, and; hence, $PbMoO_3$ is likely to contribute to the fabrication of electrode materials for fuel cells.

Thermodynamic Properties

Based on the quasi-harmonic Debye approximation[22,23] we have calculated the thermodynamic parameters like specific heat at constant volume (C_V) and thermal expansion coefficient (α) of $PbMoO_3$ under pressure and temperature variation from the calculated E–V data.

The thermodynamic properties of $PbMoO_3$ have been monitored in the temperature range of 0–

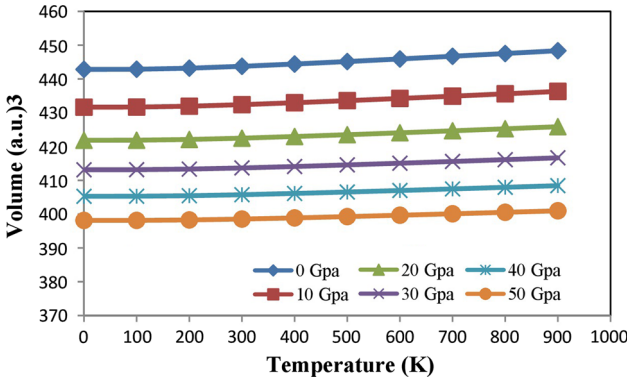

Fig. 7. Variation of unit cell volume as a function of temperature at various pressures.

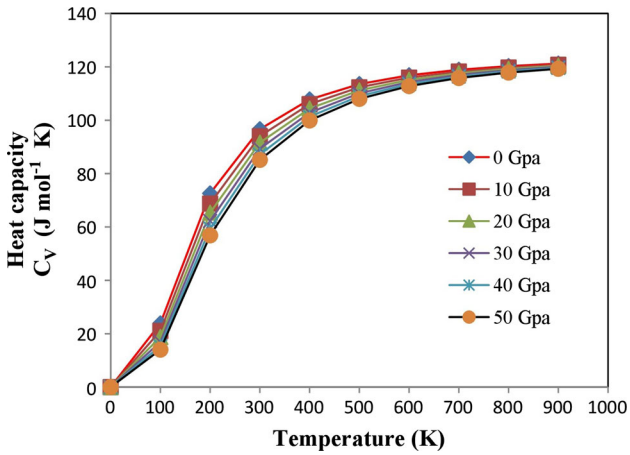

Fig. 8. Dependence of heat capacity *Cv* on temperature and pressure at constant volume.

900 K and pressure from 0 GPa to 50 GPa, where this model remains valid as we are far from the melting temperature. Figure 7 presents the variation in unit cell volume as a function of pressure and temperature. From this figure, we clearly observe that at a particular pressure the increase in temperature increases the unit cell volume and at a particular temperature the increasing pressure decreases the unit cell volume. Thus, on the one hand, temperature increases cell volume and, on the other hand, pressure decreases it, but the effect of pressure on cell volume is found more remarkable contrary to the temperature.

Specific heat (C_V) is an important thermodynamic parameter that describes the amount of heat required in processing operations. C_V provides an insight into vibrational properties compulsory for many applications. Figure 8 shows the relation of specific heat at constant volume (C_V) with respect to temperature from 0 K to 900 K and pressure from 0 Gpa to 50 GPa. From the figure, it is clear that C_V rises fast from 0 K to 450 K, but above 450 K a sluggish increase in C_V is seen, and approaches a

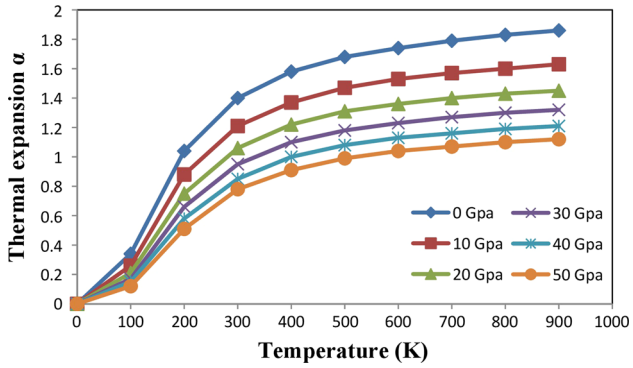

Fig. 9. Variation of thermal expansion (α) as a function of temperature at different pressure values.

constant value at a temperature of 800 K, reaching the famous Dulong- Petit limit,[46] which is common in solids. The calculated value of C_V at 300 K was found to be 96 J mol^{-1} K. For low temperatures (C_V is proportional to T^3) and beyond 800 K, C_V = 3R.

The extent to which a material expands upon heating is usually described by the coefficient of thermal expansion (α). Different materials show different trends of expansion on heating. For small temperature ranges, the (α) is proportional to change in temperature. Figure 9 shows the change in (α) with temperature and pressure, for low temperatures almost up to 300 K, (α) increases rapidly, and then a linear and slow increase in (α) is observed. Nevertheless, pressure has a reverse effect on (α), a decrease in the value of (α) is observed as pressure is increased.

CONCLUSION

In summary, the high pressure elastic, mechanical and thermodynamic properties for cubic $PbMoO_3$ have been evaluated within density functional theory (DFT). The DFT calculated structural parameters like lattice parameter at 0 GPa of pressure are in a good agreement with the available experimental and analytically calculated data. The large and increasing values of the bulk modulus and Young's modulus with increasing pressure presents the hardness and stiffness of the material and, hence, will have a potential in the fabrication of ultra-hard devices. The study also highlights the ductile nature of $PbMoO_3$. The electronic band structure and density of states presents the metallic nature of the material. Furthermore, electrical conductivity obtained by post-DFT treatment for the said compound shows a significant electrical conductivity up to 600 K. The thermodynamic investigation result provided information on unit cell volume variation, heat capacity and thermal expansion for $PbMoO_3$.

CONFLICT OF INTEREST

The authors declare that they have no conflict of interest.

REFERENCES

1. J.H. Lee and K.M. Rabe, *Phys. Rev. Lett. PRL* 104, 207204 (2010).
2. G. Srinvasan, E.T. Rasmussen, B.J. Jevin, and R. Hayes, *Phys. Rev. B* 65, 134402 (2002).
3. R.H.E. Van Doorn, H.J.M. Bouwmeester, and A.J. Burgraap, *Solid State Ion.* 111, 263 (1998).
4. M. Derras, N. Hamad, M. Derras, and A. Gessoum, *Results Phys.* 3, 219 (2013).
5. Z. Ali, I. Ahmad, I. Khan, and B. Amin, *Intermetallics* 31, 287 (2012).
6. Z. Ali, I. Khan, I. Ahmad, S. Naeem, H.A. Rahnamaye Aliabad, S.J. Asadabidi, and Z. Zhang, *Phys. B* 423, 16 (2013).
7. Z. Ali, M. Shafiq, S.J. Asadabidi, H.A. Rahnamaya, A. Abid, I. Khan, and I. Ahmad, *Comput. Mater. Sci.* 81, 141 (2014).
8. L. Soderholm, S. Skanthakumar, U. Staub, M.R. Antonio, and C.W. Williams, *J. Alloys Compd.* 250, 623 (1997).
9. C. de la Calle, J.A. Alonso, M. Garcia-Hernamdez, and V. Pomjakushin, *J. Solid State Chem.* 179, 1636 (2006).
10. M.S. Park and B.I. Min, *Phys. Rev. B* 71, 052405 (2005).
11. H.H. Wang, G.Z. Yang, D.F. Cui, H.B. Lu, T. Zhao, F. Chen, Y.L. Zhou, Z.H. Chen, Y.C. Lan, Y. Ding, L. Chen, X.L. Chen, and J.K. Liang, *J. Vac. Sci. Technol., A* 19, 930 (2001).
12. H. Takatsu, O. Hernandz, W. Yoshimune, C. Prestipino, T. Yamamato, C. Tassel, Y. Kobayashi, D. Batuk, Y. Shibata, A.M. Abakumov, C.M. Brown, and H. Kageyama, *Phys. Rev. B* 95, 155105 (2017).
13. C.R. Graves, R.R. Sudireddy, and B.M. Mogensen, *E.C.S. Transactions* 28, 173 (2010).
14. K. Kurosaki, T. Oyama, M. Hiroaki, U. Masayoshi, and Y. Shinsuke, *J. Alloys Compd.* 372, 65 (2004).
15. S. Hayashi and R. Aoki, *Mat. Res. Bull.* 14, 409 (1979).
16. G. Banarh and W.M. Temmerman, *Phys. Rev. B* 69, 054427 (2004).
17. J.G. Cheng, T. Ishii, H. Kojitani, K. Matsubayashi, A. Matsuo, X. Li, Y. Shirako, J.S. Zhou, J.B. Goodenough, C.Q. Jin, M. Akaogi, and Y. Uwatoko, *Phys. Rev. B* 88, 205114 (2013).
18. V. Cascos, J.A. Alonso, and M.T. Fernandez-Diaz, *Materials* 9, 588 (2016).
19. Z. Ali, I. Khan, I. Ahmad, M.S. Khan, and S.J. Asadabadi, *Mat. Chem. Phys.* 162, 308 (2015).
20. S.A. Khandy and D.C. Gupta, *RSC Adv.* 6, 48009 (2016).
21. P. Hohenberg and W. Kohn, *Phys. Rev. B* 64, 136 (1964).
22. X.P. Wei, Y.D. Chu, X.W. Sun, and J.B. Deng, *Eur. Phys. J. B* 86, 450 (2013).
23. S.A. Dar, V. Srivastava, and U.K. Sakalle, *J. Supercond. Novel Magn.* (2017). doi:10.1007/s10948-017-4155-9.
24. G.K. Madsen and D.J. Sing, *Comput. Phys. Commun.* 175, 67 (2006).
25. S.A. Khandy and D.C. Gupta, *Int. J. Q. Chem.* (2017). doi: 10.1002/qua.25351.
26. P. Blaha, K. Schwarz, G.K.H. Madsen, D. Kuasnicka, J. Luitz, WIEN2K, an augmented plane wave + local orbitals program for calculating crystal properties, Wien, Australia. K. Schwarz Technical Universitat; ISBN 3-9501031-1-2 (2001).
27. J.P. Perdew, K. Burke, and M. Ernzerhof, *Phys. Rev. Lett.* 77, 3865 (1996).
28. S.A. Dar, V. Srivastava, U.K. Sakalle, S. Khandy, and D.C. Gupta, *J. Supercond. Novel Magn.* (2017). doi: 10.1007/s10948-017-4181-7.
29. A.D. Becke and E.R. Johnson, *J. Chem. Phys.* 124, 221101 (2006).
30. D.D. Koelling and B.N. Harmon, *J. Phys. C Solid State* 10, 33107 (1977).
31. P.E. Blochl, O. Jepsen, and O.K. Andersen, *Phys. Rev. B* 49, 16223 (1994).
32. T. Charpin, *A Package for Calculating Elastic Tensors of Cubic Phases Using WIEN* (Paris: Laboratory of Geometrix, 2001).
33. F. Birch, *Phys. Rev.* 71, 809 (1947).
34. R. Ubic, *J. Am. Ceram. Soc.* 90, 3326 (2007).
35. R.D. Shannon, *Acta Crystallogr. Sect. A Cryst. Phys. Diffr. Theor. Gen. Crystallogr.* 32, 751 (1976).
36. J.B. Goodenough, *Rep. Prog. Phys.* 67, 1915 (2004).
37. L.E. Russel, D.L. Harrison, and N.H. Brett, *J. Nucl. Mater.* 2, 310 (1960).
38. N. Xu, H. Zhao, X. Zhou, W. Wei, X. Lu, W. Ding, and F. Li, *Int. J. Hydrogen Energy* 35, 7295 (2010).
39. S. Yousuf and D.C. Gupta, *Indian J. Phys.* 99, 31 (2017).
40. R. Hill, *Proc. Phy. Soc. Lond.* 65, 349 (1952).
41. A. Reuss and Z. Angew, *Mater. Phys.* 9, 49 (1929).
42. S.F. Pugh, *Philos. Mag.* 45, 823 (1954).
43. D.G. Pettifor, *Mater. Sci. Technol.* 8, 345 (1992).
44. E. Schreiber, O.L. Anderson, and N. Soga, *Elastic Constants and Measurements* (New York: McGraw Hill, 1973).
45. K. Bencherif, A. Yakoubi, N. Della, O.M. Abid, H. Khachai, R. Ahmad, R. Khenata, S.B. Omran, S.K. Gupta, and G. Murtaza, *J. Elec. Materials* 45, 3479 (2016).
46. A.T. Petit and P.L. Dulong, *Ann. Chim. Phys.* 10, 395 (1819).